Since January 2020 Elsevier has created a COVID-19 resource centre with free information in English and Mandarin on the novel coronavirus COVID-19. The COVID-19 resource centre is hosted on Elsevier Connect, the company's public news and information website.

Biochemical and Biophysical Research Communications 611 (2022) 190–194

Contents lists available at ScienceDirect

Biochemical and Biophysical Research Communications

journal homepage: www.elsevier.com/locate/ybbrc

Crystal structure of SARS-CoV 3C-like protease with baicalein

Jingwen Feng [a, 1], Dongyang Li [a, b, 1], Jin Zhang [c, **], Xiushan Yin [a, ***], Jian Li [b, *]

[a] Applied Biology Laboratory, College of Pharmaceutical and Biological Engineering, Shenyang University of Chemical Technology, Shenyang, 110142, China
[b] College of Pharmaceutical Sciences, Gannan Medical University, Ganzhou, 341000, China
[c] School of Basic Medical Sciences, Nanchang University, Nanchang, 330031, China

ARTICLE INFO

Article history:
Received 9 April 2022
Accepted 19 April 2022
Available online 22 April 2022

Keywords:
SARS-CoV
Baicalein
3C-like protease

ABSTRACT

The 3C-like protease (M^{pro}, $3CL^{pro}$) plays a key role in the replication process in coronaviruses (CoVs). The M^{pro} is an essential enzyme mediates CoVs replication and is a promising target for development of antiviral drugs. Until now, baicalein has been shown the specific activity for SARS-CoV M^{pro} in vitro experiments. In this study, we resolved the SARS-CoV M^{pro} with baicalein by X-ray diffraction at 2.25 Å (PDB code 7XAX), which provided a structural basis for the research and development of baicalein as an *anti*-CoVs drug.

1. Introduction

CoVs are the largest RNA viruses, which have a positive-sense, single-stranded RNA genome [1]. The severe acute respiratory syndrome (SARS) is caused by a novel species of CoVs (SARS-CoV) [2]. The symptoms of SARS-CoV infection are the lower respiratory tract disease including fever, lymphopenia, malaise and mildly elevated serum hepatic enzymes etc. [3,4]. At present, no anti-viral drugs have been found to be beneficial for SARS. The world is facing with a pandemic caused by SARS-CoV-2 now, which is a strain of CoVs spreading rapidly across the globe. But SARS-CoV-2 resulted in less widespread morbidity and mortality compared to SARS-CoV [5]. Although vaccination campaigns are underway globally, the efficacy is reduced because of the variants of concern (VOCs) [6]. Potential risk exists for SARS-CoV-2 VOCs to develop and gain some mutations similar to life threaten SARS happened in 2003. There is a need to fully understand the SARS-CoV and even the whole subtype of coronavirus.

M^{pro} is an attractive drug target among CoVs due to its essential role in processing the polyproteins which were translated from the viral RNA [7]. Studies show M^{pro} is an essential target for inhibition by interaction with Cys145 of its catalytic site [8–10]. The substrate-binding site and active site of the SARS-CoV-2 M^{pro} crystal structure in the apo state was more flexible than the ligand-binding mode [11,12]. Various complexes of the M^{pro} structure of SARS-CoV-2 with natural products and novel inhibitors have emerged. The elucidation of the mechanism of shikonin against CoVs laid the foundation for more natural products and traditional Chinese medicines as a source for antivirus drug candidates [13–15].

Flavonoids, found in various plants, are a class of polyphenolic compounds which have a structural unit of 2-phenylchromone [16]. Some flavonoid compounds have antiviral activity against CoVs by inhibiting the activity of M^{pro}. Studies showed herbacetin, gallocatechin gallate and rhoifolin can block the enzymatic activity of SARS-CoV M^{pro} due to S1, S2 and S3 sites [17,18]. Baicalein is an ingredient of Shuanghuanglian, mainly derived from the root of Scutellaria baicalensis. Baicalein shown superior binding effect to M^{pro}. Previous data showed baicalein was identified as potential noncovalent inhibitors for SARS-CoV-2 M^{pro} of IC_{50} values at 0.94 μM [19,20]. In this paper, we resolved the crystal structure of SARS-CoV M^{pro}-baicalein at 2.25 Å, analyzed and compared with the structure of SARS-CoV-2 M^{pro}-baicalein. It provides a structural basis and theoretical basis for the drug research and development of treating CoVs in the near future.

2. Materials and methods

2.1. Expression and purification of human SARS-CoV

The codon-optimized cDNAs for the SARS-CoV was synthesized fused with 6_His at the N terminus. Synthesized gene was

* Corresponding author.
** Corresponding author.
*** Corresponding author.
E-mail address: rmsl_2040@163.com (J. Li).
[1] These authors contributed equally to this work.

https://doi.org/10.1016/j.bbrc.2022.04.086
0006-291X/

Table 1
Statistics for data processing and model refinement of SARS-CoV M^{pro} with baicalein.

PDB code	7XAX
Synchrotron	SSRF
Beam line	BL02U1
Wavelength (Å)	0.97919
Space group	P1
a, *b*, *c* (Å)	55.51, 60.55, 68.28
α, *β*, *γ* (°)	90.95, 120.71, 108.65
Total reflections	129,291
Unique reflections	37,931
Resolution (Å)	2.25 (2.31–2.25)
R-merge (%)	7.1 (66.2)
Mean I/σ (I)	11.0/1.8
Completeness (%)	97.7 (96.2)
Redundancy	3.4 (3.5)
Resolution (Å)	66.31–2.25
*R*work/*R*free (%)	22.92/27.74
Atoms	4442
Mean temperature factor (Å2)	46.1
Bond lengths (Å)	0.008
Bond angles (°)	0.973
Ramachandran plot (%)	
Preferred	97.11
Allowed	2.89
outliers	0

subcloned into the pET-28a vector. The expression and purification of protease was performed by a standard method previously described [21].

2.2. X-ray crystallography

Details of the crystallization, data collection, structure solution, and refinement are provided in Table 1. Briefly, all crystallization trials were conducted using a sitting-drop vapor diffusion method at 20 °C. Baicalein was soaked with the crystal of SARS-CoV-apo within 12 h, and the X-ray diffraction data were collected at beamline02U1 (BL02U1) at the Shanghai Synchrotron Radiation Facility (SSRF, Shanghai, China). The structure solution was conducted by molecular replacement using SARS-CoV-apo (PDB code 7DQZ) as an initial model. Refinement and model building were carried out using Phenix [22] and Coot [23], respectively.

2.3. Data availability

Coordinates for SARS-CoV-M^{pro}-baicalein complexe has been deposited in the Protein Data Bank (PDB) under accession numbers 7XAX.

3. Results

3.1. Structures of SARS-CoV M^{pro}-baicalein

The binding modes of SARS-CoV M^{pro}-baicalein were compared with structure of SARS-CoV-2 M^{pro}-baicalein. In order to identify the key residues binding to baicalein, we obtained the crystal structure of SARS-CoV M^{pro} with baicalein at 2.25 Å (PDB code 7XAX) (Fig. 1A). SARS-CoV-2 M^{pro} with baicalein at 2.20 Å (PDB code 6M2N) (Fig. 1B). The structure of baicalein has been shown in (Fig. 1C). The M^{pro} of SARS-CoV and SARS-CoV-2 had 96% similarity and 95% amino acid homology [24,25]. A comparison of the sequences shows that twelve residues are different between the M^{pro} of SARS-CoV and SARS-CoV-2 (Fig. 1D).

3.2. Crystal structure of SARS-CoV M^{pro} with baicalein

The protomer is composed of three domains. Domain I and domain II have an antiparallelβ-barrel structure. Domain III contains five α-helices arranged into a largely antiparallel globular cluster, and it is connected to domain II by a long loop region [13](Fig. 2A). From the structure of SARS-CoV M^{pro}, the S2 and S2′subsites are critical for substrate binding to the SARS-CoV M^{pro} [26–28]. SARS-CoV M^{pro} with baicalein had a Cys145-His41 catalytic dyad in the S2 subsite, which located in a cleft between domain I and domain II [19,29–31](Fig. 2B). SARS-CoV M^{pro} with baicalein is shown in (Fig. 2C). Three phenolic hydroxyl groups of baicalein form hydrogen bonds with the main chains of Cys145/Ser144/Gly143 as well as the side chains of Asn142/Asn141. The free benzene ring inserted into S2 subsite by making hydrophobic interactions with multiple residues Gln189/Arg188/Glu166/Met165/His164/Asp48/His41. With the aid of an array of direct hydrogen bonds with Cys145/Ser144/Gly143, baicalein served to stabilize the tetrahedral transition state of the proteolytic reaction (Fig. 2D).

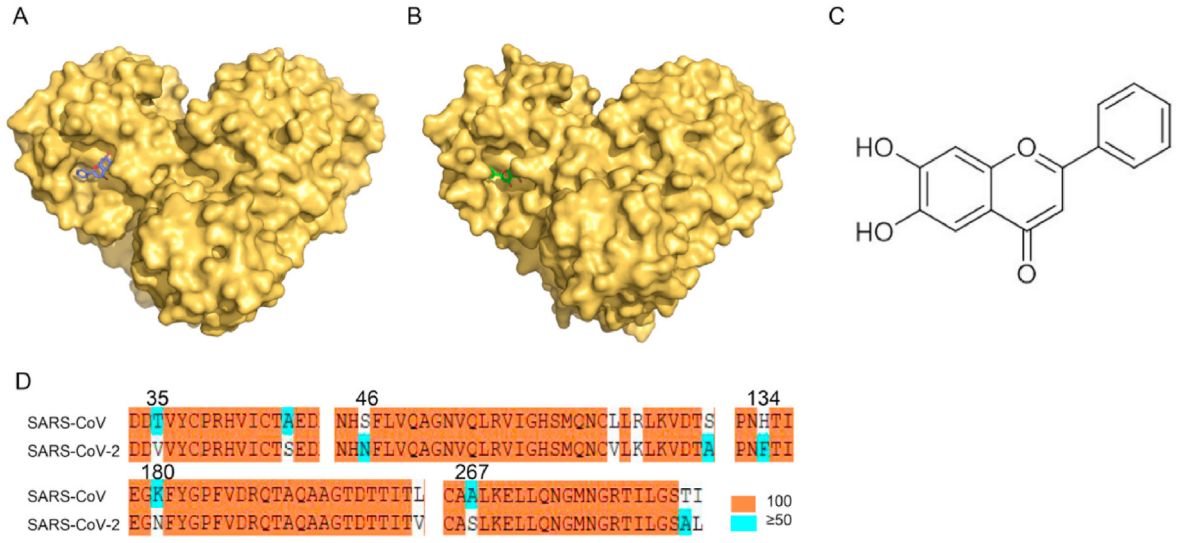

Fig. 1. Comparison of the binding pocket of M^{pro} from different CoVs. (A) Surface of SARS-CoV M^{pro}. Baicalein is shown in purple. Oxygen atoms are shown in red. (B) Surface of SARS-CoV-2 M^{pro}. Baicalein is shown in green. Oxygen atoms are shown in red. (C) The structure of baicalein. (D) Alignment of the M^{pro} of SARS-CoV and SARS-CoV-2. The conserved precent has been shown orange (100),blue (≥50). (For interpretation of the references to color in this figure legend, the reader is referred to the Web version of this article.)

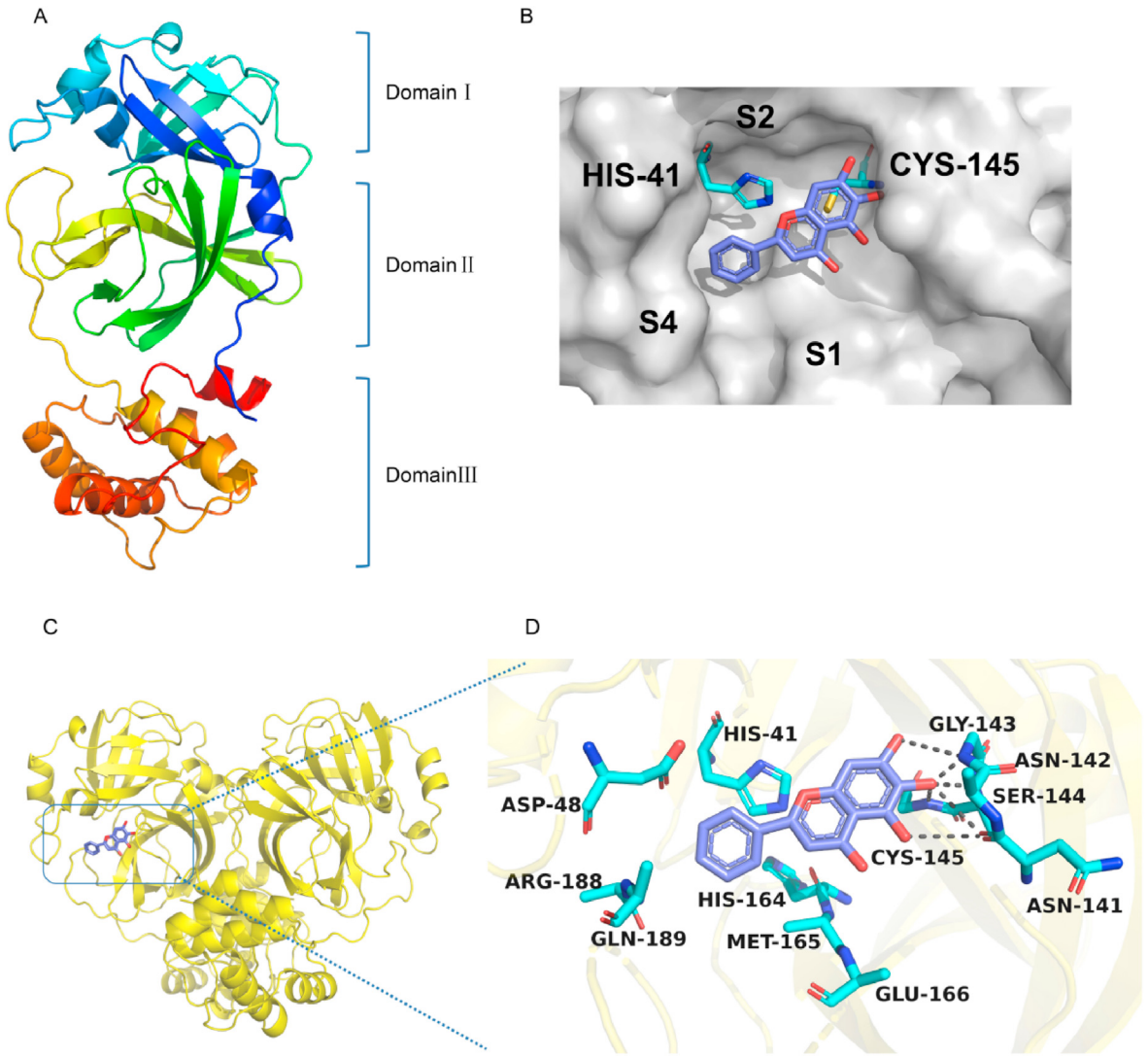

Fig. 2. Crystal structure of SARS-CoV M^{pro} with baicalein (PDB code7XAX). (A) Overview of homodimers shown as cartoon. (B) The binding pocket of SARS-CoV M^{pro} with baicalein. Baicalein is shown in purple. (C) The structure of SARS-CoV M^{pro} with baicalein. SARS-CoV is shown in yellow and baicalein is shown in purple. Oxygen atoms are shown in red. (D) Interactions of SARS-CoV with baicalein (purple). Residues as well as the baicalein are shown as sticks and hydrogen bonds are represented by dashed lines. (For interpretation of the references to color in this figure legend, the reader is referred to the Web version of this article.)

3.3. Comparison of structure of SARS-CoV M^{pro}-baicalein and SARS-CoV-2 M^{pro}-baicalein

SARS-CoV M^{pro} and SARS-CoV-2 M^{pro} have the same binding mode with baicalein, both have the binding sites include the Cys145-His41 catalytic dyad (Fig. 3A and D). Baicalein in the active site of SARS-CoV M^{pro} and SARS-CoV-2 M^{pro} (Fig. 3B and E). The phenolic hydroxyl group of baicalein in SARS-CoV M^{pro} forms hydrogen bonds with mains chains and side chains has been shown in (Fig. 3D). The SARS-CoV-2 M^{pro} with baicalein complexes are hydrogen-bonded to the Ser144/Gly143/Leu141 and side chains via the water molecule, where the only carbonyl group established a hydrogen bond with the main chain of Glu166 [32–34]. The free benzene ring also inserted into the S2 subsite by hydrophobic interactions with His41 residue (Fig. 3F). The electrostatic potential surface surrounding the active pocket in SARS-CoVs with baicalein are also shown in Fig. 3. It was revealed that SARS-CoV-apo (Fig. 3G) is different from that of SARS-CoV M^{pro}-baicalein(Fig. 3H). SARS-CoV-2-apo (Fig. 3I) is different from SARS-CoV-2 M^{pro}-baicalein (Fig. 3J).

4. Discussion

Recently, as the cases of SASR-CoV-2 infections, the effective drugs and vaccines has already been found [35]. But there are currently no antivirus drugs approved for the prevention or treatment of highly virulent SARS-CoV infection. M^{pro} plays a key role involved in the replication and transcription of CoVs among the few available targets for *anti*-CoVs drugs, which has become an essential and relatively mature drug target in *anti*-CoVs drug research. M^{pro} inhibitors mainly exhibit reversible binding with the amino acid residues in S1, S2, and S4 pockets. The inhibitors contain unsymmetrical aromatic disulphides showing inhibitory activity including the flavonoids compounds [36].

Flavonoid compounds displayed good inhibition toward M^{pro} [37]. Correspondingly, baicalein which belongs to flavonoid compounds has been shown the specific activity for SARS-CoV M^{pro} in vitro experiments. SARS-CoV M^{pro} has a Cys145-His41 catalytic dyad in the cleft between domains I and II, can recognize the eleven cleavage sites of nsp4-16 specifically and exhibit self-hydrolytic cleavage activity [38]. Here, we resolved the crystal structure of

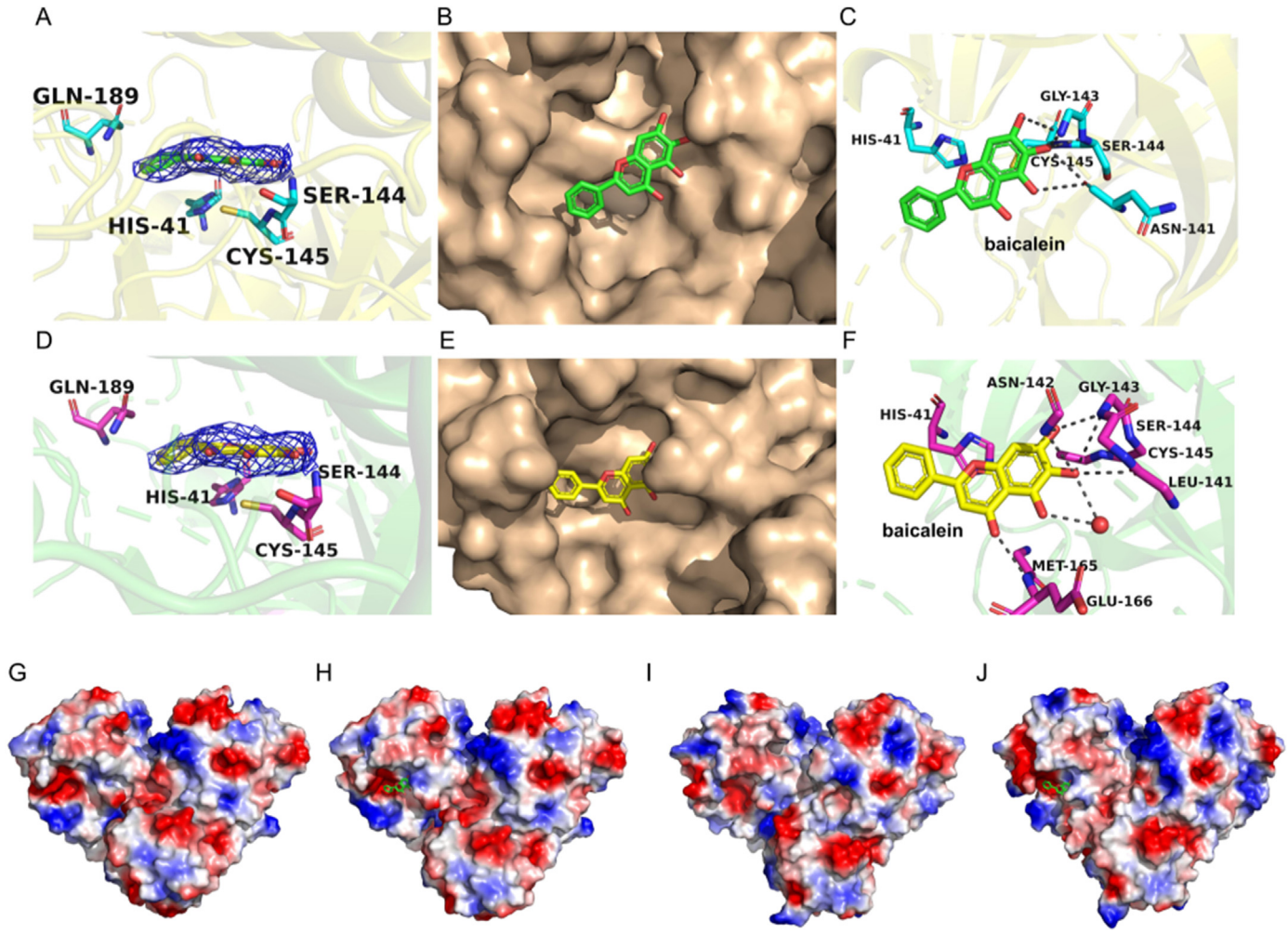

Fig. 3. Crystal structures of SARS-CoVs with baicalein. (A) Electron density maps (2Fo-Fc) of baicalein at 1.0 σ (7XAX). (B) Baicalein (green) in the active site of SARS-CoV M^{pro}. (C) Hydrogen bonding (dashed lines) interactions between SARS-CoV M^{pro} and baicalein. (D) Electron density maps (2Fo-Fc) of baicalein at 1.0 σ (6M2N). (E) Baicalein (yellow) in the active site of SARS-CoV-2 M^{pro}. (F) Hydrogen bonding (dashed lines) interactions between SARS-CoV-2 M^{pro} and baicalein. (G) Electrostatic potential surface distribution of SARS-CoV-apo. (H) Electrostatic potential surface distribution of SARS-CoV M^{pro}-baicalein. (I) Electrostatic potential surface distribution of SARS-CoV-2-apo. (J) Electrostatic potential surface distribution of SARS-CoV-2 M^{pro}-baicalein. The color of the surface denotes the electrostatic potential, while red signifiies negative charge and blue signifiies positive charge. Baicalein is shown in sticks (green). (For interpretation of the references to color in this figure legend, the reader is referred to the Web version of this article.)

SARS-CoV M^{pro} with baicalein that can bind to the substrate pocket between domain I and domain II. Three phenolic hydroxyl groups of baicalein make hydrogen bonds with the main chains of Cys145/Ser144/Gly143 as well as the side chains of Asn142/Asn141, providing a structural basis and theoretical basis for baicalein to inhibit the replication of SARS-CoV.

Declaration of competing interest

The authors have no conflicts of interest to declare.

Acknowledgements

This work was supported by Jiangxi natural science Foundation for distinguished young scholar (20212ACB216001), Gannan Medical University (QD201910), Jiangxi key research and development program (20203BBG73063) and Jiangxi "Double Thousand Plan (jxsq2019101064)", Central government funds for guiding local scientific and Technological Development(2021JH6/10500225), Construction of Liaoning technological innovation center (1590826279052).

Appendix A. Supplementary data

Supplementary data to this article can be found online at https://doi.org/10.1016/j.bbrc.2022.04.086.

References

[1] Perlman Stanley, A. Dandekar Ajai, Immunopathogenesis of coronavirus infections: implications for SARS, Nat. Rev. Immunol. 5 (2005) 917–927. https://www.ncbi.nlm.nih.gov/pmc/articles/PMC7097326.
[2] Joseph S.M. Peiris, Kwok Y. Yuen, Albert D.M. E. Osterhaus, et al., The severe acute respiratory syndrome, N. Engl. J. Med. 349 (2003) 2431–2441. https://pubmed.ncbi.nlm.nih.gov/14681510.
[3] Satija Namita, K. Lal Sunil, The molecular biology of SARS coronavirus, Ann. N. Y. Acad. Sci. 1102 (2007) 26–38. https://pubmed.ncbi.nlm.nih.gov/17470909.
[4] J.S.M. Peiris, Y. Guan, K.Y. Yuen, Severe acute respiratory syndrome, Nat. Med. 10 (2004) S88–S97. https://www.ncbi.nlm.nih.gov/pmc/articles/PMC7096017.
[5] K.B. Anand, S. Karade, S. Sen, et al., SARS-CoV-2SARS-CoV-2: camazotz's curse, Med. J. Armed Forces India 76 (2020) 136–141. https://pubmed.ncbi.nlm.nih.gov/32341622.
[6] Shapira Tirosh, Monreal I. Abrrey, P. Dion Sébastien, et al., A TMPRSS2 inhibitor acts as a pan-SARS-CoV-2 prophylactic and therapeutic, Nature (2022). Mar 28, https://pubmed.ncbi.nlm.nih.gov/35344983.
[7] Linlin Zhang, Daizong Lin, Xinyuanyuan Sun, et al., Crystal structure of SARS-CoV-2 main protease provides a basis for design of improved α-ketoamide

inhibitors, Science (2020) 368. https://pubmed.ncbi.nlm.nih.gov/32198291.
[8] Kidera Akinori, Moritsugu Kei, Ekimoto Toru, et al., Allosteric regulation of 3CL protease of SARS-CoV-2 and SARS-CoV observed in the crystal structure ensemble, Mol. Biol. 433 (2021), 167324. https://pubmed.ncbi.nlm.nih.gov/34717972.
[9] J. Niesor Eric, Boivin Guy, Rhéaume Eric, et al., Inhibition of the 3CL protease and SARS-CoV-2 replication by dalcetrapib, ACS Omega 6 (2021) 16584–16591. https://pubmed.ncbi.nlm.nih.gov/34235330.
[10] Zhenming Jin, Yao Zhao, Yuan Sun et al Structural basis for the inhibition of SARS-CoV-2 main protease by antineoplastic drug carmofur, Nat. Struct. Mol. Biol. 27, 529–532. https://pubmed.ncbi.nlm.nih.gov/32382072.
[11] Zhenming Jin, Xiaoyu Du, Yechun Xu, et al., Structure of M(pro) from COVID-19 virus and discovery of its inhibitors, Nature 582 (2020) 289–293. https://pubmed.ncbi.nlm.nih.gov/32272481.
[12] Xuelan Zhou, Fanglin Zhong, Lin Cheng, et al., Structure of SARS-CoV-2 main protease in the apo state, Sci. China Life Sci. 64 (2021) 656–659. https://pubmed.ncbi.nlm.nih.gov/32880863.
[13] Riddhidev Banerjee, Lalith Perera, L.M. Viranga Tillekeratne, Potential SARS-CoV-2 main protease inhibitors, Drug Discov. Today (2021 Mar). https://pubmed.ncbi.nlm.nih.gov/33309533.
[14] Li Jian, Xuelan Zhou, Yan Zhang, et al., Crystal structure of SARS-CoV-2 main protease in complex with the natural product inhibitor shikonin illuminates a unique binding mode, Sci. Bull. 66 (2021) 661–663. https://pubmed.ncbi.nlm.nih.gov/33163253.
[15] Yuting Zhang, Hongxia Gao, Xiaohui Hu, et al., Structure-Based discovery and structural basis of a novel broad-spectrum natural product against the main protease of coronavirus, J. Virol. 96 (2022), e0125321. https://pubmed.ncbi.nlm.nih.gov/34586857.
[16] Kangmei Wen, Xiaochuan Fang, Junli Yang, et al., Recent research on flavonoids and their biomedical applications, Curr. Med. Chem. 28 (2021) 1042–1066. https://pubmed.ncbi.nlm.nih.gov/32660393.
[17] Seri Jo, Suwon Kim, Dong Hae Shin, Mi-Sun Kim, Inhibition of SARS-CoV 3CL protease by flavonoids, Enzyme Inhib. Med. Chem. (2020 Dec). https://pubmed.ncbi.nlm.nih.gov/31724441.
[18] Thi Thanh Hanh Nguyen, Hye-Jin Woo, Hee-Kyoung Kang, et al., Flavonoid-mediated inhibition of SARS coronavirus 3C-like protease expressed in Pichia pastoris, Biotechnol. Lett. 34 (2012) 831–838. https://pubmed.ncbi.nlm.nih.gov/22350287.
[19] Hai-Xia Su, Sheng Yao, Wen-Feng Zhao, et al., Anti-SARS-CoV-2 activities in vitro of Shuanghuanglian preparations and bioactive ingredients, Acta Pharmacol. Sin. 41 (2020) 1167–1177. https://pubmed.ncbi.nlm.nih.gov/32737471.
[20] Dafu Zhu, Haixia Su, Changqiang Ke, et al., Efficient discovery of potential inhibitors for SARS-CoV-2 3C-like protease from herbal extracts using a native MS-based affinity-selection method, Pharm. Biomed. Anal. 209 (2022 Feb 5), 114538. https://pubmed.ncbi.nlm.nih.gov/34929567.
[21] H. Gao, Y. Zhang, H. Jiang, et al., Crystal structures of human coronavirus NL63 main protease at different pH values, Acta Crystallogr. F Struct. Biol. Commun. (2021 Oct). https://pubmed.ncbi.nlm.nih.gov/34605439.
[22] D. Adams Paul, W. Grosse-Kunstleve Ralf, Wei Hung Li, et al., PHENIX: building new software for automated crystallographic structure determination, Acta Crystallogr. D Biol. Crystallogr. 58 (2002) 1948–1954. https://pubmed.ncbi.nlm.nih.gov/12393927.
[23] Emsley Paul, Cowtan Kevin, Coot: model-building tools for molecular graphics, Acta Crystallogr. D Biol. Crystallogr. 60 (2004) 2126–2132. https://pubmed.ncbi.nlm.nih.gov/15572765.
[24] Kanchan Anand, Ziebuhr John, Wadhwani Parvesh, et al., Coronavirus main proteinase (3CLpro) structure: basis for design of anti-SARS drugs, Science 300 (2003) 1763–1767. Science.2003, https://pubmed.ncbi.nlm.nih.gov/12746549.
[25] Archisha Prakash, Borkotoky Subhomoi, Dubey Vikash Kumar, Targeting two potential sites of SARS-CoV-2 main protease through computational drug repurposing, J. Biomol. Struct. Dyn. (2022) 1–11, undefined, https://pubmed.ncbi.nlm.nih.gov/35266856.
[26] Yao Zhao, Yan Zhu, Xiang Liu, et al., Structural basis for replicase polyprotein cleavage and substrate specificity of main protease from SARS-CoV-2, Proc. Natl. Acad. Sci. U. S. A. 119 (2022), e2117142119. https://pubmed.ncbi.nlm.nih.gov/35380892.
[27] Xiaoyu Xue, Haitao Yang, Wei Shen, et al., Production of authentic SARS-CoV M(pro) with enhanced activity: application as a novel tag-cleavage endopeptidase for protein overproduction, J. Mol. Biol. 366 (2007) 965–975. https://pubmed.ncbi.nlm.nih.gov/17189639.
[28] A.S. Achutha, V.L. Pushpa, Suchitra Surendran, Theoretical insights into the anti-SARS-CoV-2 activity of chloroquine and its analogs and in silico screening of main protease inhibitors, J. Proteome Res. 19 (2020) 4706–4717. https://pubmed.ncbi.nlm.nih.gov/32960061.
[29] W. Dai, B. Zhang, X.M. Jiang, et al., Structure-based design of antiviral drug candidates targeting the SARS-CoV-2 main protease, Science 368 (2020) 1331–1335. https://pubmed.ncbi.nlm.nih.gov/32321856.
[30] M. Yuan, N.C. Wu, X. Zhu, A highly conserved cryptic epitope in the receptor binding domains of SARS-CoV-2 and SARS-CoV, Science (2020 May 8). https://pubmed.ncbi.nlm.nih.gov/32245784.
[31] Zumla Alimuddin, F.W. Chan Jasper, I. Azhar Esam, et al., Coronaviruses-drug discovery and therapeutic options, Nat. Rev. Drug Discov. 15 (2016) 327–347. https://pubmed.ncbi.nlm.nih.gov/26868298.
[32] Pavlova Anna, L. Lynch Diane, Daidone Isabella, et al., Inhibitor binding influences the protonation states of histidines in SARS-CoV-2 main protease, Chem. Sci. 12 (2021) 1513–1527. https://pubmed.ncbi.nlm.nih.gov/35356437.
[33] L. Zhang, D. Lin, X. Sun, et al., Crystal structure of SARS-CoV-2 main protease provides a basis for design of improved a-ketoamide inhibitors, Science 368 (2020) 409–412. https://pubmed.ncbi.nlm.nih.gov/32198291.
[34] Antonopoulou Io, Sapountzaki Eleftheria, Rova Ulrika, et al., Inhibition of the main protease of SARS-CoV-2 (M) by repurposing/designing drug-like substances and utilizing nature's toolbox of bioactive compounds, Comput. Struct. Biotechnol. J. 20 (2022) 1306–1344. https://pubmed.ncbi.nlm.nih.gov/35308802.
[35] Mohanraj Dinesh, Whitelegg Alison, Trilogy of COVID-19: infection, vaccination, and immunosuppression, Int. Arch. Allergy Immunol. (2022) 1–19, undefined, https://pubmed.ncbi.nlm.nih.gov/35390803.
[36] Yuzhi Liu, Chengyuan Liang, Xin Liang, et al., The development of Coronavirus 3C-Like protease (3CL) inhibitors from 2010 to 2020, Eur. J. Med. Chem. 206 (2020), 112711. https://www.ncbi.nlm.nih.gov/pmc/articles/PMC7409838.
[37] Seri Jo, Suwon Kim, Dae Yong Kim, et al., Flavonoids with inhibitory activity against SARS-CoV-2 3CLpro, Enzyme Inhib. Med. Chem. 35 (2020) 1539–1544. https://pubmed.ncbi.nlm.nih.gov/32746637.
[38] Keqiang Fan, Ma Liang, Xiaofeng Han, et al., The substrate specificity of SARS coronavirus 3C-like proteinase, Biochem. Biophys. Res. Commun. 329 (2005) 934–940. https://www.ncbi.nlm.nih.gov/pmc/articles/PMC7092912.